*Journal of Statistical Physics, Vol. 54, Nos. 1/2, 1989*

# A Numerical Study of the Phase Structure of the $q$-State Generalization of the Hard-Square Model

**Tobias M. Haas**[1]

*Received January 6, 1987; revision received August 9, 1988*

An investigation is made of how a recently found $q$-state generalization of the hard-square model fits into a more general phase diagram. The investigation is done by Monte Carlo and series expansion methods. Evidence is presented that the one-dimensional manifold of parameters along which the model is exactly solvable represents a line of first-order phase transitions.

**KEY WORDS:** Exactly solvable models; hard-square model; $q$ species; IRF model; commuting transfer matrices; Monte Carlo simulation; series expansion.

## 1. INTRODUCTION

Two-dimensional lattice models in statistical mechanics are studied for many reasons: First there is Onsager's celebrated exact solution of the two-dimensional Ising model[1] that revolutionized the theory of phase transitions. Since then a number of other models have been exactly solved[2,3] which are now seen as representatives of the most important universality classes describing phase transitions in two dimensions.[4,5] This is of great significance, since one-dimensional systems with short-range interactions do not have singular behavior at finite (nonzero) temperatures, whereas the combinatorics in three dimensions has so far not yielded to exact solutions but in two exceptional cases.

Exact solutions therefore seem to be limited, at least for the time being, to two dimensions. Notwithstanding this limitation, much we know about critical phenomena has been learned from these models. Also, in recent years refined experimental techniques have made it possible to study

[1] Institute for Theoretical Physics, State University of New York at Stony Brook, Stony Brook, New York 11794-3840.



0022-4715/89/0100-0201$06.00/0 

physical systems in two dimensions, such as surfaces of metals and alloys or adsorbed monolayers of gases on such surfaces.[7,8]

In most cases exactly solved models are too restricted to fully describe physical systems. There are, however, powerful approximate techniques, such as series expansions and Monte Carlo simulations, which allow one to treat more general systems and make predictions that can be tested experimentally.

The hard-core lattice gas is an example of such a system: Its phase structure was originally studied by Gaunt and Fisher.[9,10] This study, using series expansion techniques, later prompted an exact solution by Baxter within the hard-square lattice gas.[11] Fisher and Gaunt's results can also be used to make predictions about a number of physical systems (such as adsorption of Cl on Ag(100)[8]. Originally the interest in various types of lattice gases had been concentrated on the character of the liquid–solid and gas–liquid phase transitions.[12] The aim was to determine what properties of the intermolecular potential drive the first-order phase transition. These properties are now fairly well understood, and work on these systems focuses on other goals. One of these goals is to bring the exact results in line with predictions made by the conformal bootstrap program.[4,5,13] The other, as mentioned above, is to apply the results to physical systems.

All of this makes this class of models very interesting. In addition, the pursuit of exact solutions of generalizations of the hard-square model has led to a number of new combinatorial theorems[14,15] related to the Rogers–Ramanujan identities. There exist essentially two different types of generalizations: One is the ABF hierarchy of Andrews *et al.*[3] Here the restriction of the hard-square model is written as

$$0 \leqslant \sigma_i + \sigma_j \leqslant 1 \qquad (\sigma_i, \sigma_j = 0, 1) \tag{1}$$

where $i$ and $j$ are neighboring sites. This restriction is then generalized to[14,15]

$$k-1 \leqslant \sigma_i + \sigma_j \leqslant k \qquad (\sigma_i, \sigma_j = 0,..., k) \tag{2}$$

(For convenience I restrict myself here to the $r =$ odd cases of the ABF hierarchy.) Further relaxation of (2) to

$$0 \leqslant \sigma_i + \sigma_j \leqslant k \tag{3}$$

also leads to exactly solvable cases.[14–16,18]

Another type of generalization starts from the condition

$$\sigma_i \sigma_j = 0, \qquad \sigma_i, \sigma_j = 0, 1,..., q \tag{4}$$

Condition (4) with $q=1$ is equivalent to condition (1). Generalizations of type (4) have been made by a number of authors.[19–22] Models of type (4) have an immediate physical interpretation: The site variable $\sigma_i = l$ stands for a hard-square particle of species $l$ occupying site $i$. Nearest neighbor sites cannot be occupied simultaneously. There are $q$ different species overall. The model allows for anisotropic next nearest neighbor interactions.

The hard-square model ($q=1$) has been studied extensively,[11,23–26] and I shall not get back to it here. Also, the case $q=2$ has been studied in detail.[20,21] I therefore turn to the case of condition (4) with $q \geqslant 3$, for which a commuting family of transfer matrices has been obtained.[22] This family is parametrized in terms of one spectral parameter and has no temperature-like variable. It is different from both Baxter's $q=1$ and Pearce *et al.*'s $q=2$ cases. The purpose of this paper is to understand how this new exact solution fits into a larger phase diagram that contains all the other known solutions. The analysis is done by Monte Carlo methods and series expansions.

The results of the computer simulations indicate that the one-dimensional exactly solvable manifold of the $q$-species hard-square model (which I shall call $E_L$ from here on) is a first-order coexistence curve. On this line a homogeneous solid (a $\sqrt{2} \times \sqrt{2}$ densely packed state of one type of particle only) coexists with a gaseous phase (a low-density disordered phase containing all types of particles with equal probability).

The results here presented are not exact. However, the mutual agreement of Monte Carlo results with exact predictions on $E_L$ and of the series with the Monte Carlo results away from $E_L$ makes the evidence very strong.

In the following main section of this paper I first define the model. I then present the results of the simulation and of the series expansion. I end with an outlook on what else this combination of methods could be used for.

## 2. DEFINITIONS

The model I am considering is an extended version of the one discussed in ref. 22. The model is defined on a two-dimensional square lattice with periodic boundary conditions in the IRF language.[2] Each lattice site can be occupied by one out of $q$ different species of particles denoted by $\sigma_i = 1,..., q$. If the site $i$ is unoccupied, $\sigma_i = 0$. Neighboring sites cannot be occupied simultaneously. This model can be interpreted graphically in the following fashion (Fig. 1): Hard-square particles of $q$ different species live on the sites of a two-dimensional square lattice; particles cannot overlap,

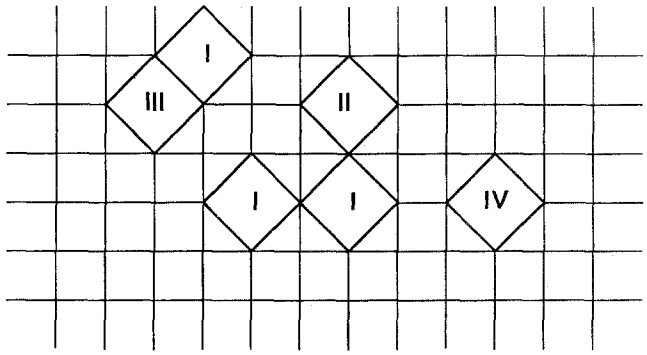


Fig. 1. Typical low-density configuration for $q = 4$.

implying an infinite nearest neighbor repulsion, and particles that touch interact (next nearest neighbor interaction). Phrased in the IRF language, the model is given in terms of Boltzmann weights defined on plaquettes (Fig. 2). The weights $\omega_1$, $\omega_2(i)$, $\omega_3(i)$, $\omega_4(i)$, $\omega_5(i)$, $\omega_6(i, j)$, and $\omega_7(i, j)$ can in principle depend on $i$ and $j$ $(i \neq j)$ as long as they obey the restrictions $\omega_6(i, j) = \omega_6(j, i)$ and $\omega_7(i, j) = \omega_7(j, i)$.

In this paper I do not consider weights $\omega$ with $i, j$ dependence. The Yang–Baxter equations have not been solved under these general assumptions. However, for the case that the weights are independent of $i$ and $j$ a number of solutions are known (Jimbo and Miwa's families *TI*, *TII*, *EI*, and *EII* for $q = 2$, a case which reduces trivially to the $q = 1$ hard-

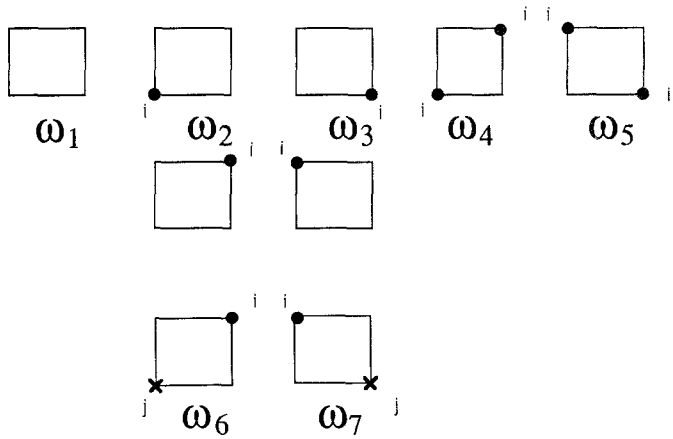


Fig. 2. Definition of the face weights.

square model and the case $E_L$ for $q \geqslant 3$.) To be specific, I shall consider weights of the following form:

$$\begin{gathered} \omega_1 = 1, \qquad \omega_2 = z, \qquad \omega_3 = z \\ \omega_4 = z^2 e^L, \qquad \omega_5 = z^2 e^M, \qquad \omega_6 = z^2 e^{\tilde{L}}, \qquad \omega_7 = z^2 e^{\tilde{M}} \end{gathered} \tag{5}$$

The parameter $z$ acts as a fugacity. (To be more precise, each particle on the lattice contributes a factor $z^4$ to the partition function.) $-L$ is the interaction energy between identical particles across SW–NE diagonals ($-M$ for SE–NW diagonals, respectively); $-\tilde{L}$ and $-\tilde{M}$ are the interaction energies of differing particles across the two diagonals, respectively. In this notation $E_L$ is described by the following equations (the variable $x$ ranges between 1 and $q-1$):

$$\begin{aligned} z &= \left(\frac{q-1}{q}\right)^{1/4} \frac{\{(x-1)[(q-1)/x-1]\}^{1/2}}{q-2} \\ x_1 &= \frac{(q-2)[(q-1)-x/(q-1)]}{(x-1)^2} \\ x_2 &= \frac{(q-2)[(q-1)-1/x]}{[(q-1)/x-1]^2} \\ y_1 &= \frac{q-2}{x-1} \\ y_2 &= \frac{q-2}{(q-1)/x-1} \end{aligned} \tag{6}$$

where

$$x_1 = e^L, \qquad x_2 = e^M, \qquad y_1 = e^{\tilde{L}}, \qquad y_2 = e^{\tilde{M}}$$

For comparison I also give the corresponding expressions for the hard-hexagon model and the cases $E$ and $T$ of Jimbo and Miwa (note that their two families in each case, namely $E_\pm$ and $T_\pm$, can be obtained by interchanging $x_2$ and $y_2$; they are all contained in the following expressions).

Hard hexagons:

$$\begin{aligned} &\alpha = \beta = 0 \\ &z = q^{-1/4}\left[\frac{(1-1/x_1)(1-1/x_2)}{x_1 x_2 - x_1 - x_2}\right]^{1/4} \end{aligned} \tag{7}$$

*EI*, *EII* ($q=2$):

$$x_1=\frac{\alpha+\beta}{\beta(1-\alpha^2)^{1/2}}, \qquad x_2=\frac{\alpha+\beta}{\alpha(1-\beta^2)^{1/2}}$$
$$z=\frac{1}{2^{1/4}}\frac{[\alpha\beta(1-\alpha^2)(1-\beta^2)(1+\alpha\beta)]^{1/4}}{\alpha+\beta} \tag{8}$$

*TI*, *TII* ($q=2$):

$$x_1=\frac{(1-\alpha^2)^{1/2}}{\beta^2}, \qquad x_2=\frac{(1-\beta^2)^{1/2}}{\alpha^2}, \qquad z=\frac{1}{2^{1/4}}(\alpha\beta)^{1/2}$$

In all three cases $\alpha$ and $\beta$ are given by

$$\alpha=\frac{x_1 y_1-1}{x_1 y_1+1}, \qquad \beta=\frac{x_2 y_2-1}{x_2 y_2+1} \tag{9}$$

Comparing these four expressions, the differences between the four families can clearly be seen. The solution manifolds for *H*, *EI*, *EII*, *TI*, and *TII* are two dimensional, while $E_L$ is one dimensional. It is also clear that $E_L$ is not a submanifold of either of the other three families: $E_L$ is only defined for $q \geqslant 3$, while *E* and *T* are defined for $q=2$ only. *H* is defined for all values of *q*. However, $E_L$ and *H* only intersect in two points, the left and the right shift points. $E_L$ therefore represents a distinct new solution manifold. In particular, due to the fact that $E_L$ is one dimensional, there is no temperature-like variable on $E_L$. These observations lead to three questions which I shall try to answer in the following section:

1. Is $E_L$ a locus of phase transition points?
2. Of what nature are these phase transition points?
3. How reliable are the predictions concerning 1 and 2?

I shall try to answer these questions in the following three sections.

## 3. IS $E_L$ A LOCUS OF PHASE TRANSITION POINTS?

In order to study the model away from $E_L$, I vary *z* [as defined in (5)] around $z_L$, its value on $E_L$. Proceeding from small to larger values of *z* one expects at some point to encounter a phase transition from a gaseous to a solid phase. In this particular case this means that one goes from a low-density random arrangement of particles to a densely packed state. Due to the hard-core repulsion of the particles, they arrange themselves on

either one of the two sublattices in the ordered phase (Fig. 4). Along the entire solvable line $E_L$ the interactions are attractive and in addition the interactions between identical particles are much stronger than the ones between different particles. To be more specific, consider two states $A$ and $B$. State $A$ is a densely packed configuration of identical particles and state $B$ is identical to state $A$, except that one particle in the bulk is replaced by one of a different type. For the total weights $W_A$ and $W_B$ of these two configurations, i.e., the products of all the face weights of each state, one gets the following estimate, which is valid for all values of $x$ and $q$:

$$\frac{W_A}{W_B} = \frac{\omega_4^2 \omega_5^2}{\omega_6^2 \omega_7^2} \gtrsim 100 \tag{10}$$

This means that the ordered phase will be a homogeneous solid, i.e., consisting of one type of particle only. The order parameters relevant in this transition are given by

$$r_i = \frac{\rho_A(i) - \rho_B(i)}{2} \tag{11}$$

where $\rho_A(i)$ and $\rho_B(i)$ are the densities of particles of type $i$ on sublattices $A$ and $B$, respectively. For values of $z > z_c$, i.e., in the ordered regime, one expects $q$ ordered phases coexisting with one disordered phase. For the $j$th ordered phase $r_1, \ldots, r_{j-1}, r_{j+1}, \ldots, r_q = 0$ and $r_j = 0$. Since this model is symmetric with respect to permutation of particle type, it is only necessary to study the combination

$$R = \sum_{j=1}^{q} [r_A(j) - r_B(j)] \tag{12}$$

I performed this study using Monte Carlo techniques. Monte Carlo simulations are well established in statistical physics and extensive literature exists on this subject.[41–54] I believe, however, that this is the first study of this type performed on an IRF model with strong constraints reducing the space of allowed states. There are complications associated with using the Monte Carlo method on these systems since it is not *a priori* clear that the algorithm properly samples the entire energy surface. While it is known that the algorithm is ergodic for spin systems,[41] one cannot make such a statement here. Results therefore have to be considered with greater care.

It is for this reason that I have used a series expansion of the particle density to check the validity of the Monte Carlo results. I also stress at this point that the numerical calculations have been done for the case $q = 3$

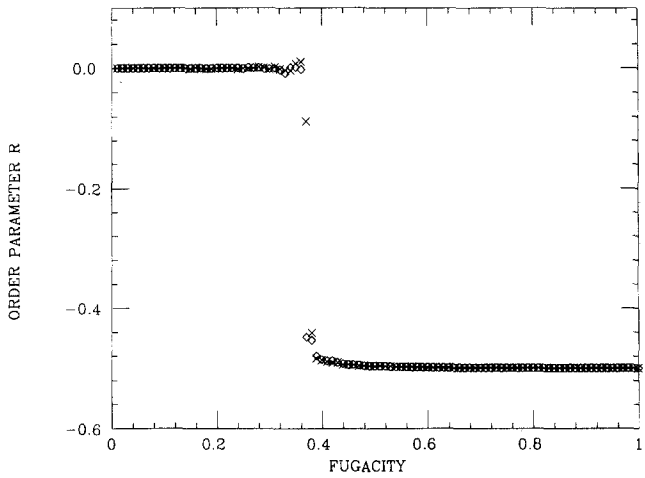


Fig. 3. Order parameter $R$ vs. fugacity $z$, $x = \sqrt{2}$, $14 \times 14$ lattice.

only. The qualitative features of the model do not vary with $q$; the numerical values of course do. This is a different situation from the $q$-state Potts model, where the parametrization of the weights is different for $q = 3, 4$ and $q > 4$.

Figure 3 shows a typical result of a simple simulation. The simulation was done for a $14 \times 14$ lattice and a value of $x = \sqrt{2}$. The figure shows the results for the order parameter as a function of the parameter $z$ defined in Eq. (5). The result looks strongly indicative of a phase transition at one particular value $z = z_c$. Table I displays the values $z = z_L$ that correspond to $E_L$, the exactly solvable manifold. [Note that the values of $x$ range between 1 and $(q-1)^{1/2}$ only, since replacing $x \to (q-1)/x$ merely rotates

**Table I. The Values of $z_c$ as Found by the MC Simulation for Various Lattice Sizes and Values of $x$, the Spectral Parameter[a]**

| Lattice size | $x = 1.1$ | $x = 1.2$ | $x = 1.3$ | $x = \sqrt{2}$ | $x = 1.5$ |
|---|---|---|---|---|---|
| $8 \times 8$ | 0.251 | 0.333 | 0.348 | 0.365 | 0.363 |
| $10 \times 10$ | 0.256 | 0.319 | 0.350 | 0.368 | 0.370 |
| $12 \times 12$ | 0.259 | 0.330 | 0.360 | 0.371 | 0.365 |
| $14 \times 14$ | 0.260 | 0.320 | 0.356 | 0.365 | 0.370 |
| $16 \times 16$ | 0.259 | 0.327 | 0.360 | 0.372 | 0.368 |
| $17 \times 17$ | 0.258 | 0.330 | 0.368 | 0.375 | 0.375 |
| $18 \times 18$ | 0.252 | 0.320 | 0.360 | 0.374 | 0.369 |

[a] The values of $z_c$ all carry an error of approximately $\pm 0.010$.

**Table II. Exact Values, to Three Decimals, of $z_L$, Describing the Exactly Solvable Manifold $E_L$, as a Function of the Spectral Parameter $x$[a]**

| $x$ | 1.1 | 1.2 | 1.3 | $\sqrt{2}$ | 1.5 |
|---|---|---|---|---|---|
| $z_c$ | 0.259 | 0.330 | 0.363 | 0.374 | 0.369 |

[a] The values of $z_c$ of the Table I agree within error bars with $z_L$.

the lattice by 90°. The results are therefore reflection invariant around $x=(q-1)^{1/2}$] For comparison the values of the transition fugacities $z=z_c$ are listed in Table II for various values of $x$ and various lattice sizes. These results from a simple simulation on small lattices already indicate the existence of a phase transition and give the location to be on the exactly solvable line. These results also seem to indicate that the transition is of first order. However, a more detailed analysis is necessary to settle the question of the existence and the order of the transition. I shall present this analysis in the next section.

## 4. OF WHAT NATURE ARE THE PHASE TRANSITION POINTS ALONG $E_L$?

Recently Challa *et al.*[27,28] have suggested a finite-size analysis for first-order transitions. Although their analysis is phenomenological in nature, it makes very accurate predictions for the Ising model and for the Potts model. I have applied their method to the present problem and find that the results are consistent with the assumption that the phase transition is of first order.

If the present model exhibits a first-order transition, one expects discontinuities in the internal energy, the density, and the quantity $R$ defined in the previous section. These discontinuities are reflected in $\delta$-function singularities in the specific heat, the compressibility, and the staggered compressibility. In the finite system under consideration in the simulation the singularities are rounded and shifted. Careful analysis of how the rounding and shifting occur as functions of the size of the lattice allows one to extrapolate to the thermodynamic limit.

In particular, Challa *et al.* have considered a quantity of the type

$$V_L = 1 - \frac{\langle D^4 \rangle}{3\langle D^2 \rangle^2} \tag{13}$$

From a phenomenological analysis they deduce the following behavior for $V_L$:

1. In the disordered regime, far away from the phase transition, $V_L \to 2/3$ as $L \to \infty$.

2. At the transition point in the finite system $z_L^v V_L$ has a minimum. At a second-order phase transition this minimum disappears as $L \to \infty$. At a first-order transition the minimum persists and the approach of the minimum value to the limiting value is linear in $1/L^2$.

I have studied quadratic square lattices of linear dimensions 10, 18, 26, 30, 34, and 40 for the case $q=3$ and $x=\sqrt{2}$. I have monitored the quantities $V_L$, the specific heat, and the compressibility.

Examples of the results for a lattice of $26 \times 26$ sites are shown in Figs. 4 – 6. The minimum in Fig. 4 deepens and narrows as the size of the lattice increases. The maxima in Figs. 5 and 6 increase and narrow similarly with increasing lattice size. The location of the maxima and the minimum also move with the size of the lattice. The most significant result is shown

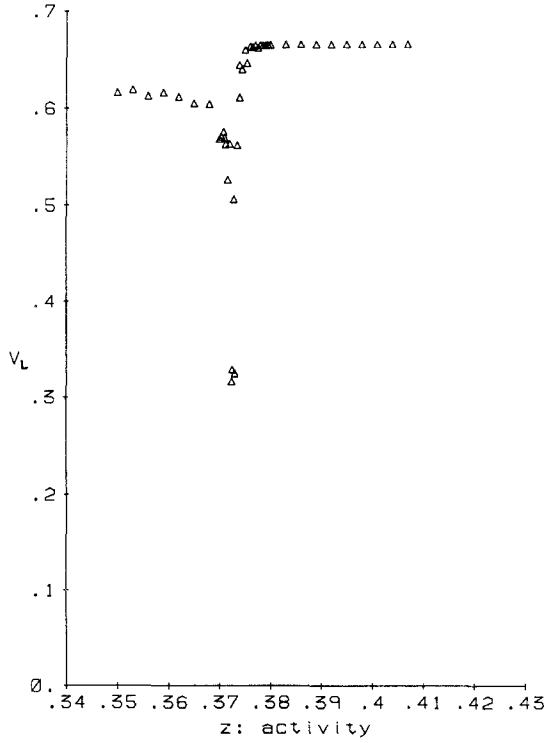


Fig. 4. Quantity $V_L$ vs. fugacity $z$, $x=\sqrt{2}$, $26 \times 26$ lattice.

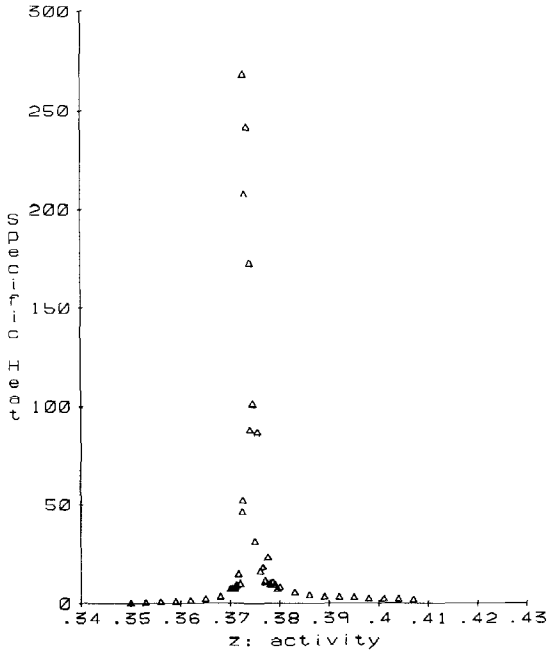


Fig. 5. Specific heat vs. fugacity $z$, $x = \sqrt{2}$, $26 \times 26$ lattice.

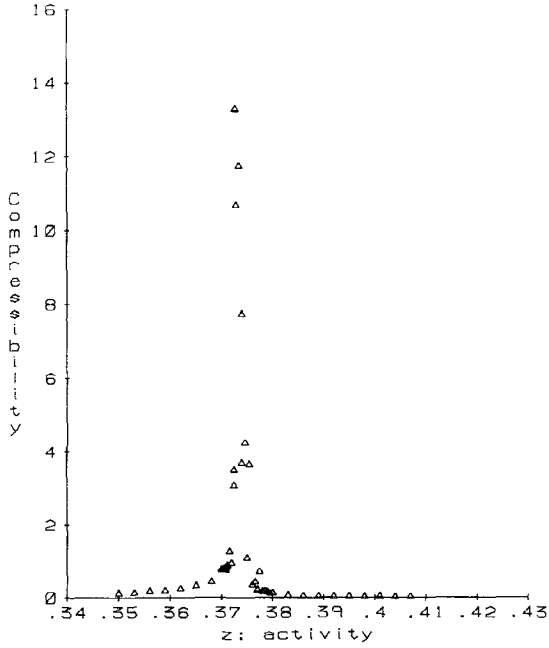


Fig. 6. Compressibility vs. fugacity $z$, $x = \sqrt{2}$, $26 \times 26$ lattice.

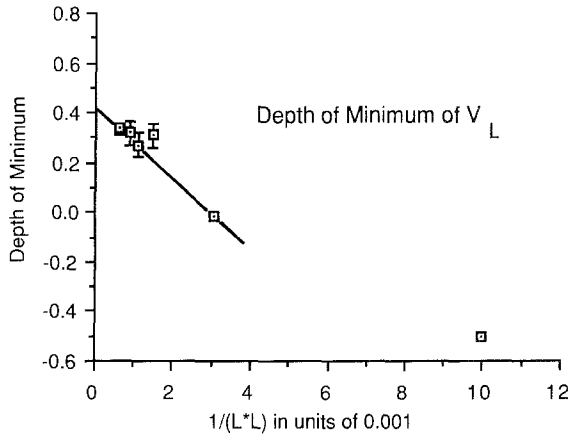


Fig. 7. Depth of minima of $V_L$ vs $1/L^2$. Note the linear approach to a value less than 2/3.

in Fig. 7. There I plot the depth of the minimum of $V_L$ versus $1/L^2$. According to refs. 27 and 28, this function should become linear for larger and larger lattices and at a first-order transition extrapolate to a value less than 2/3 as $L \to \infty$. At a second-order transition the function extrapolates to 2/3. The results in Fig. 7 are consistent with this picture and, most importantly, they show that the minimum of $V_L$ persists as $L \to \infty$. This is so since the line extrapolates to a value that is clearly less than 2/3.

It is necessary to mention here that $V_L$ contains the fourth-order moment of the density distribution. It is particularly hard to calculate such a high moment of the distribution and a calculation requires very large numbers of iterations. Challa *et al.* report that they achieved a time of 1.6 $\mu$sec per update. My Fortran program running on a Ridge 32 minicomputer took 320 $\mu$sec per update. The maximum number of iterations that was feasible was $10^5$/lattice site. The results therefore have large statistical errors but they are accurate enough to exclude the second-order transition.

I have also plotted the locations of the minima of $V_L$ and the maxima of the specific heat and the compressibility as well as the heights of these peaks (Figs. 8–12). It is important for the present argument that these quantities scale with the volume $V = L^2$ of the system (or $1/V$, respectively) as is typical for a first-order transition.[29–34] In a second-order transition one would see anomalous exponents related to $\nu$, the exponent of the correlation length.[35–40],[2]

[2] See ref. 38 for a recent review on finite-size scaling.

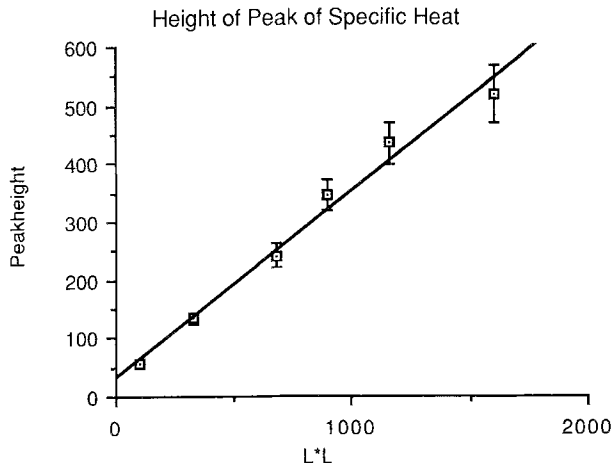


Fig. 8. Height of peaks of specific heat vs. $L^2$.

## 5. HOW VALID ARE THE RESULTS?—SERIES EXPANSIONS

Finally, I address the question of whether the results of the Monte Carlo simulation can be trusted. I point out here that ref. 48 deals with a similar task, namely to verify the first-order character of the transition in the $Q > 4$ Potts model. There also the second derivatives seem to diverge so that no hysteresis loop is seen.

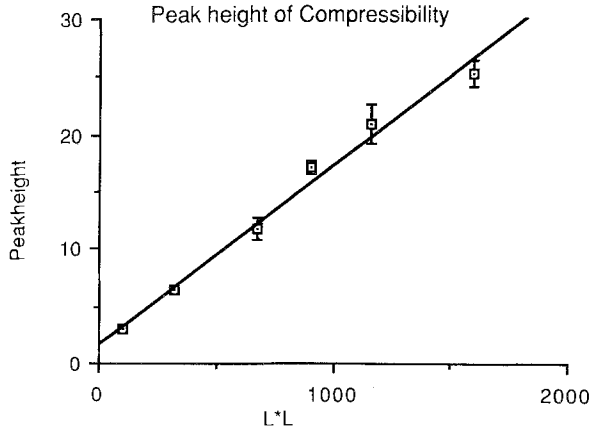


Fig. 9. Height of peaks of compressibility vs. $L^2$.

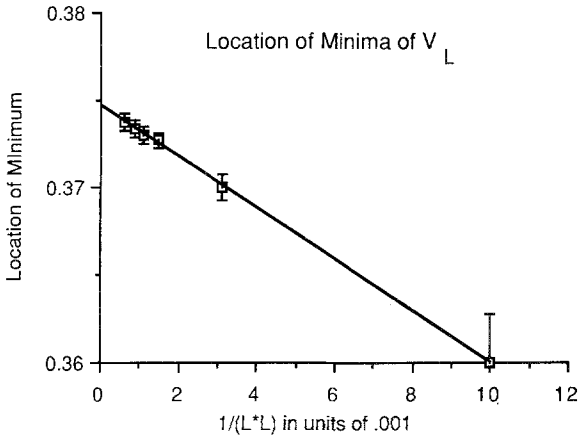


Fig. 10. Location of minima of $V_L$ vs. $1/L^2$.

It is straightforward to obtain the first few terms in a low- and a high-density expansion in this model. The results are given by

$$\rho = qz^4(1 + a_1 z^4 + a_2 z^8 + a_3 z^{12} + \cdots) \tag{14}$$

in the low-density phase and

$$\rho = \frac{1}{2}\left(1 + \frac{A_1}{z^4} + \frac{A_2}{z^8} + \frac{A_3}{z^{12}} + \cdots\right) \tag{15}$$

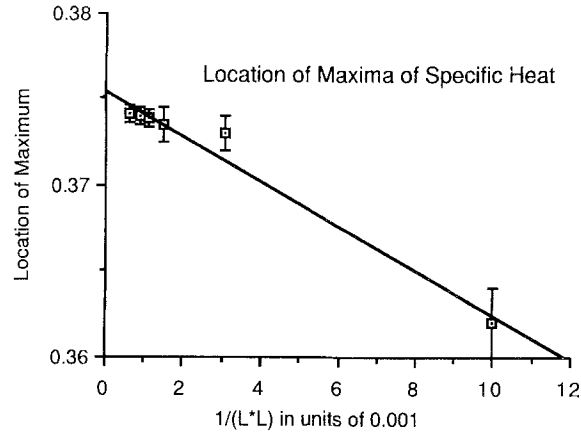


Fig. 11. Location of maxima of specific heat vs. $1/L^2$.

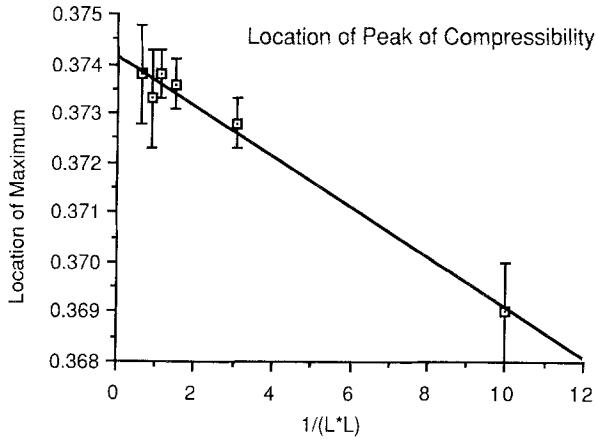


Fig. 12. Location of maxima of compressibility vs. $1/L^2$.

in the high-density phase. The coefficients $a_i$ and $A_i$ are polynomials in $x_1, x_2, y_1, y_2$, and $q$. These polynomials are listed in the Appendix. Figure 13 shows an example of how well the series and the Monte Carlo data agree.

Finally, since the Monte Carlo results confirm the theoretical predic-

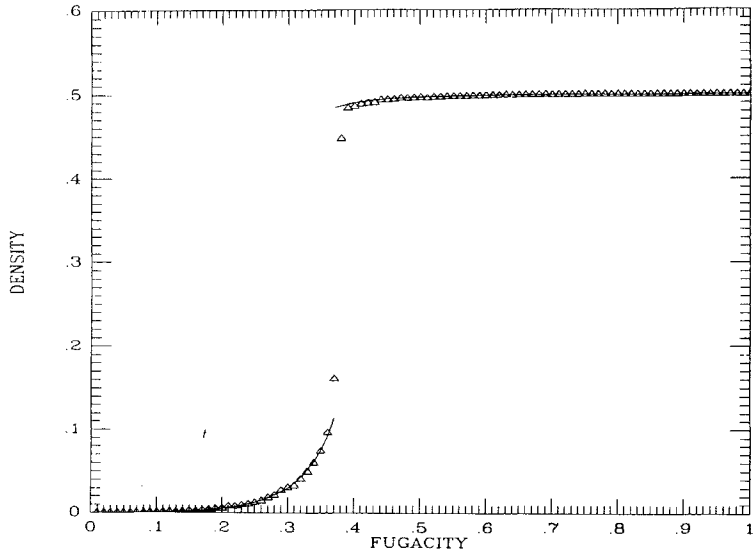


Fig. 13. Series vs. Monte Carlo. MC from $14 \times 14$ lattice, 1000 iterations per lattice site, $x = \sqrt{2}$.

tions and the series expansions in turn verify the Monte Carlo data, I feel confident about the Monte Carlo results. I further believe that the data support the hypothesis that $E_L$ is a first-order coexistence curve. I remark here that the expression for the free energy of this model is identical to the one of the $Q$-state Potts model, where $q$ and $Q$ are related by

$$Q_{\text{Potts}} = \frac{q^2}{q-1} \tag{16}$$

So the present case ($q=3$) would correspond to the $Q=9/2$ Potts model.

## 6. CONCLUSION

I believe I have given strong evidence that the exactly solvable line $E_L$ of the $q$-state generalization of the hard-square model is a first-order coexistence curve. This fact is in itself interesting since there exists a belief that on an exactly solvable first-order manifold the Boltzmann weights are parametrizable in terms of hyperbolic functions. The classic example for this is the Potts model, where for $Q \leqslant 4$ the parametrization is trigonometric and for $Q > 4$ hyperbolic. This model would furnish another example where this belief is true.

I have applied a finite-size scaling method recently suggested by Challa *et al.* This method is based on a phenomenological approach, but it gives very accurate answers for the Potts model. In this case the method predicts that the phase transition is of first order. There are also theoretical indications that this should be the case. So this new method not only strengthens my argument, it also proves itself. To appreciate this, one should note that the model considered here has a property that sets it apart from the Potts model, namely, it has a large number of forbidden states. It is not *a priori* clear that the Monte Carlo method should work in this model at all, but apparently it does. Also, that Challa *et al.*'s analysis works is a nontrivial observation.

At this point there are two avenues to persue: First, one might try to calculate some more quantities exactly, such as the discontinuities across $E_L$. Maybe this study provides enough hints to go about such a calculation. Second, the method used here can be applied to other lattice systems, in particular the case $q=2$.[20] I believe that this is a particularly interesting case: The weights are less restricted there since some conditions are trivially satisfied. Correspondingly, one finds weights parametrized in

terms of elliptic functions; the exactly solvable manifold is simply much larger. Also, this model lends itself very naturally to applications.

Altogether I believe that numerical methods naturally extend exact solutions. The exact results in turn provide milestones against which numerical results can be checked. More often than not, numerical results alone leave considerable doubt as to their validity and accuracy.

## APPENDIX

The expressions for the series coefficients $a_i$ and $A_i$ are

$$a_1 = 2\left(s + t - \frac{9}{2}q\right)$$

$$a_2 = 3\left(s^2 + t^2 + 4st - 14q(s+t) + \frac{97}{3}q^2\right)$$

$$a_3 = 4\left\{s^3 + t^3 + 8s^2t + 8st^2 - 19q(s^2+t^2) - 39qst - \frac{57}{2}q(s^2+t^2)\right.$$
$$+ \frac{181}{2}q(s+t) + [x_1x_2 + (q-1)\,y_1y_2]^2 + (q-1)$$
$$\left.\times [x_1y_2 + x_2y_1 + (q-2)\,y_1y_2]^2 + \frac{837}{2}q^3\right\}$$

where $s = x_1 + (q-1)\,y_1$ and $t = x_2 + (q-2)\,y_2$ and

$$A_1 = -\left(\frac{1}{x_1^2x_2^2} + (q-1)\left\{2\left(\frac{1}{x_1y_1x_2^2} + \frac{1}{x_1^2x_2y_2} - \frac{5}{x_1^2x_2^2}\right)\right.\right.$$
$$+ 2[\sigma^2 + \tau^2 + (q-2)(\sigma\tau^2 + \sigma^2\tau)]\left(\frac{1}{x_1y_1x_2^2} + \frac{1}{x_2y_2x_1^2} - \frac{4}{x_1^2x_2^2}\right)$$
$$+ 2\tau^2[\sigma(q-2)-1]\left(\frac{1}{x_1^2x_2y_2}\right) + 2\sigma^2[\tau(q-2)+1]\frac{1}{x_1y_1x_2^2}\Big\}\sigma^2\tau^2$$
$$+ (q-1)^2\left[\frac{31}{x_1^2x_2^2} - 16\left(\frac{1}{x_1y_1x_2^2} + \frac{1}{x_1^2x_2y_2}\right) + \frac{1}{x_1^2y_2^2} + \frac{1}{x_2^2y_1^2}\right.$$
$$\left.\left.+ \frac{4}{x_1y_1x_2y_2}\right]\sigma^4\tau^4\right)$$

$$A_2 = -2\left(\frac{1}{x_1^3 x_2^3}\left(\frac{1}{x_1}+\frac{1}{x_2}-\frac{5}{2}\frac{1}{x_1 x_2}\right)+(q-1)\,\sigma^2\tau^2\right.$$
$$+\left\{\left(\frac{1}{x_2^2 y_1^2}+\frac{1}{x_1^2 y_2^2}+\frac{2}{y_1 x_2^2}+\frac{2}{y_2 x_1^2}\right)\frac{1}{x_1^2 x_2^2}\right.$$
$$+\frac{1}{x_1^3 x_2^3}\left[4\left(\frac{1}{y_1}+\frac{1}{y_2}\right)-4\left(\frac{1}{y_1 x_2}+\frac{1}{y_2 x_1}\right)\right.$$
$$\left.\left.\left.-8\left(\frac{1}{x_1}+\frac{1}{x_2}\right)+\frac{4}{y_1 y_2}\right]+\frac{61}{x_1^4 x_2^4}\right\}\right)$$
$$A_3 = -3\left\{\frac{1}{x_1^4 x_2^4}\left(\frac{1}{x_1^2}+\frac{1}{x_2^2}\right)+\frac{1}{x_1^5 x_2^5}\left[4-8\left(\frac{1}{x_1}+\frac{1}{x_2}\right)\right]+\frac{31}{3}\frac{1}{x_1^6 x_2^6}\right\}$$

where $\sigma = y_1/x_1$ and $\tau = y_2/x_2$.

## ACKNOWLEDGMENTS

I would like to thank my advisor, Jacques H. H. Perk, for considerable help with this problem and Gregory A. Kohring for many useful suggestions concerning the Monte Carlo simulation. I would also like to acknowledge David Huse, who pointed me to the work of Challa, Landau, and Binder and who provided many other useful comments.

This work was supported in part through NSF grant DMR-85-05419.

## REFERENCES

1. L. Onsager, *Phys. Rev.* **65**:117 (1944).
2. R. J. Baxter, *Exactly Solved Models in Statistical Mechanics* (Academic Press, London, 1982).
3. G. E. Andrews, R. J. Baxter, and P. J. Forrester, *J. Stat. Phys.* **35**:193 (1984).
4. A. A. Belavin, A. B. Zamolodchikov, and A. M. Polyakov, *J. Stat. Phys.* **34**:763 (1984).
5. D. Friedan, Z. Qiu, and S. Shenker, *Phys. Rev. Lett.* **52**:1575 (1984).
6. D. A. Huse, *Phys. Rev. B* **30**:3908 (1984).
7. G. A. Somorjai, *Chemistry in Two Dimensions* (Cornell University Press, 1981).
8. I. Jäger, *Vacuum* **31**:531 (1981).
9. D. S. Gaunt and M. E. Fisher, *J. Chem. Phys.* **43**:2840 (1965).
10. D. S. Gaunt, *J. Chem. Phys.* **46**:3237 (1967).
11. R. J. Baxter, *J. Phys. A* **13**: L61 (1981).
12. L. K. Runnels, in *Phase Transitions and Critical Phenomena*, Vol. 2, C. Domb and M. S. Green, eds. (Academic Press, London).
13. M. Jimbo, T. Miwa, and M. Okado, *Nucl. Phys. B* **257[FS17]**:517 (1986).
14. R. J. Baxter and G. E. Andrews, *J. Stat. Phys.* **44**:249 (1986).
15. R. J. Baxter and G. E. Andrews, *J. Stat. Phys.* **44**:713 (1986).

16. Y. Akutsu, A. Kuniba, and M. Wadati, *J. Phys. Soc. Jpn.* **55**:1092, 1466, 1980, 2166, 2605 (1986).
17. Y. Akutsu, A. Kuniba, and M. Wadati, *Phys. Lett. A* **117**:358 (1986).
18. P. J. Forrester and G. E. Andrews, *J. Phys. A* **19**: L923 (1986).
19. M. Jimbo and T. Miwa, *Physica D* **15**:335 (1985).
20. M. Jimbo and T. Miwa, *Nucl. Phys. B* **257[FS14]**:1 (1985).
21. P. A. Pearce, *J. Phys. A* **18**:3217 (1985).
22. T. M. Haas and J. H. H. Perk, Stony Brook Preprint; T. M. Haas, Ph. D. Thesis, State University of New York at Stony Brook (1987).
23. D. A. Huse, *J. Phys. A* **16**:4357 (1983).
24. D. A. Huse, *Phys. Rev. Lett.* **49**:1121 (1982).
25. R. J. Baxter and P. A. Pearce, *J. Phys. A* **15**:807 (1982).
26. R. J. Baxter and P. A. Pearce, *J. Phys. A* **16**:2230 (1983).
27. K. Binder and D. P. Landau, *Phys. Rev. B* **30**:1477 (1984).
28. M. S. S. Challa, D. P. Landau, and K. Binder, *Phys. Rev. B* **34**:1841 (1986).
29. Y. Imry, *Phys. Rev. B* **21**:2042 (1980).
28. M. E. Fisher and A. N. Berker, *Phys. Rev. B* **26**:2507 (1982).
30. V. Privman and M. E. Fisher, *J. Stat. Phys.* **33**:385 (1983).
31. J. L. Cardy and M. P. Nightingale, *Phys. Rev. B* **27**:4256 (1983).
32. K. Binder and D. P. Landau, *Phys. Rev. B* **30**:1477 (1984).
33. V. Privman and M. E. Fisher, *J. Appl. Phys.* **57**:3327 (1985).
34. A. E. Ferdinand and M. E. Fisher, *Phys. Rev.* **185**:3832 (1969).
35. M. E. Fisher and M. N. Barber, *Phys. Rev. Lett.* **28**:1516 (1972).
36. M. P. Nightingale, *Physica* **83A**:561 (1976).
37. D. P. Landau, *Phys. Rev. B* **13**:2997 (1976); **14**:225 (1976).
38. M. N. Barber, in *Phase Transitions and Critical Phenomena*, C. Domb and J. L. Lebowitz, eds. (Academic Press, New York, 1983), p. 145.
39. K. Binder, in *Phase Transitions and Critical Phenomena*, vol. 9 (Academic Press, New York, 1983), p. 1.
40. N. Metropolis, A. W. Rosenbluth, M. N. Rosenbluth, A. H. Teller, and E. Teller, *J. Chem. Phys.* **21**:1087 (1953).
41. C. P. Yang, *Proc. Symp. Appl. Math.* **15**:351 (1963).
42. J. M. Hammersley and D. C. Handscomb, *Monte Carlo Methods* (Methuen, London, 1964).
43. K. Binder, in *Phase Transitions and Critical Phenomena*, vol. 3 (Academic Press, New York, 1976).
44. K. Binder (ed.), *Monte Carlo Methods* (Springer-Verlag, Berlin, 1979).
45. C. Rebbi, *Lattice Gauge Theories and Monte Carlo Simulations* (World Scientific, Singapore, 1983).
46. K. Binder (ed.), *Applications of the Monte Carlo Method* (Springer-Verlag, Berlin, 1984).
47. K. Binder, *J. Stat. Phys.* **24**:69 (1981).
48. B. J. Adler and T. E. Wainwright, *J. Chem. Phys.* **31**:459 (1959).
49. B. J. Adler and T. E. Wainwright, *J. Chem. Phys.* **33**:1439 (1960).
50. B. J. Adler and T. E. Wainwright, *Phys. Rev.* **127**:359 (1962).
51. W. W. Wood and J. D. Jacobson, *J. Chem. Phys.* **27**:720 (1957).
52. W. W. Wood and J. D. Jacobson, *J. Chem. Phys.* **27**:1207 (1957).
53. W. W. Wood, F. R. Parker, and J. D. Jacobson, *Nuovo Cimento* **9** (Suppl. 1):133 (1958).